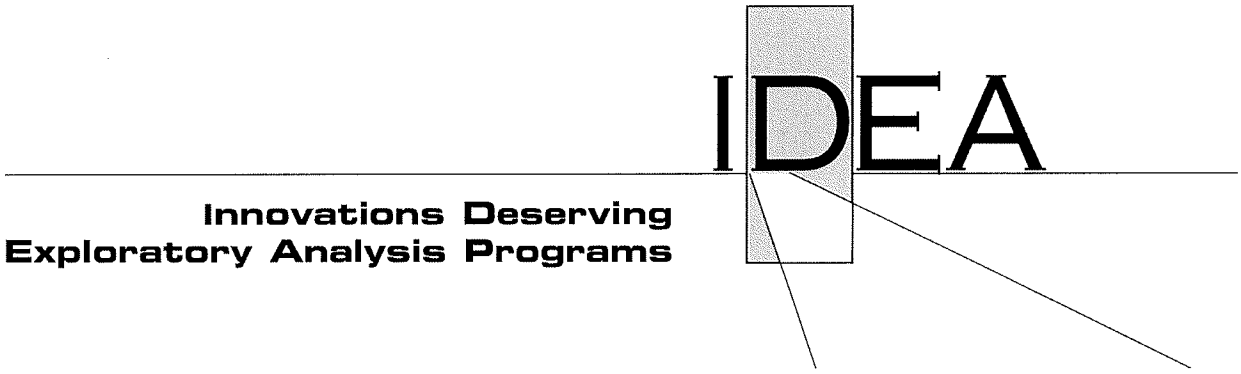

Highway IDEA Program

Digital Specimen and Multiple Functional Digital Tester Technique for Performance Evaluation of Asphalt Mixes

Final Report for Highway IDEA Project 122

Prepared by:
Linbing Wang
Virginia Polytechnic Institute and State University
Blacksburg, VA

February 2008

TRANSPORTATION RESEARCH BOARD
OF THE NATIONAL ACADEMIES

INNOVATIONS DESERVING EXPLORATORY ANALYSIS (IDEA) PROGRAMS MANAGED BY THE TRANSPORTATION RESEARCH BOARD (TRB)

This NCHRP-IDEA investigation was completed as part of the National Cooperative Highway Research Program (NCHRP). The NCHRP-IDEA program is one of the four IDEA programs managed by the Transportation Research Board (TRB) to foster innovations in highway and intermodal surface transportation systems. The other three IDEA program areas are Transit-IDEA, which focuses on products and results for transit practice, in support of the Transit Cooperative Research Program (TCRP), Safety-IDEA, which focuses on motor carrier safety practice, in support of the Federal Motor Carrier Safety Administration and Federal Railroad Administration, and High Speed Rail-IDEA (HSR), which focuses on products and results for high speed rail practice, in support of the Federal Railroad Administration. The four IDEA program areas are integrated to promote the development and testing of nontraditional and innovative concepts, methods, and technologies for surface transportation systems.

For information on the IDEA Program contact IDEA Program, Transportation Research Board, 500 5th Street, N.W., Washington, D.C. 20001 (phone: 202/334-1461, fax: 202/334-3471, http://www.nationalacademies.org/trb/idea).

DIGITAL SPECIMEN AND MULTIPLE FUNCTIONAL DIGITAL TESTER TECHNIQUE FOR PERFORMANCE EVALUATION OF ASPHALT MIXES

Final Report

Principal Investigator
Linbing Wang, Ph.D., P.E., Associate Professor
Civil and Environmental Engineering Department
Virginia Polytechnic Institute and State University
Associate Director, CSTI, Virginia Tech Transportation Institute

February 2008

TABLE OF CONTENTS

LIST OF FIGURES

LIST OF TABLES

SUMMARY

This report summarizes the work completed under NCHRP-IDEA 122 project. The project goal was to develop a 3-D digital representation of the microstructure of an asphalt concrete specimen and an asphalt mastic specimen and evaluating the performance of the 'digital specimens' using modeling and simulation techniques. Therefore, the final product would be a computer program that reads processed computed-tomography images, reconstructs them into "digital specimens", and performs the stiffness test on them using the platform of a Finite Element code. The work was accomplished in two phases.

In the first phase, a computer program to represent the microstructure of cylindrical specimens of asphalt concrete and mastic in digital format (digital specimen) and modules to link their microstructure to a finite element code for simulating the indirect tensile test and dynamic modulus test (digital test) were developed. The simulation models used elastic and viscoplastic material models for aggregate and asphalt respectively. By using rate dependent material model for asphalt binder, the numerical simulation of the indirect tensile test provided realistic response for the asphalt mixture when qualitatively compared with the experimental results. The model successfully captured the stress variation resulting from the presence of both aggregates and voids, and the test was able to distinguish performance differences of different mixes used in the evaluation. Work was also performed on the development of a method for parameter estimation using inverse algorithm based on simulation results and test data. The viscoplastic model for asphalt binder was refined and used to conduct realistic digital tests with the microstructure of the asphalt concrete mixture and mastic. Based on the comparison of simulated and observed test results, realistic models were selected and integrated into the digital specimen interface modules to generate a multi-functional digital "tester."

In phase two, an attempt to implement the digital specimen and digital test technique at the FHWA's Turner-Fairbank Research Center will be made. Implementation needs to be conducted through training programs and workshops for demonstrating their applications in performance evaluation of asphalt concrete.

1. INTRODUCTION

Simple performance tests are used to characterize the viscoelastic material properties in pavement design. Indirect tensile test and dynamic modulus test (Figure 9) are widely used to predict the mechanical properties of asphalt concrete in terms of resilient modulus, phase angle and dynamic modulus. In practice, the interpretation of the test is simplified using elasticity. For indirect tensile test, the simplified theoretical solutions for the plane stress condition along the horizontal and vertical diameters (Hondros 1959) are usually used to obtain stresses (Figure 1). This is mainly due to the complex geometry of the specimen and the difficulty of obtaining a theoretical solution for a viscoplastic material. For dynamic modulus test, uniaxial loading with uniform stress distribution is assumed to interpret stresses and strains in the sample.

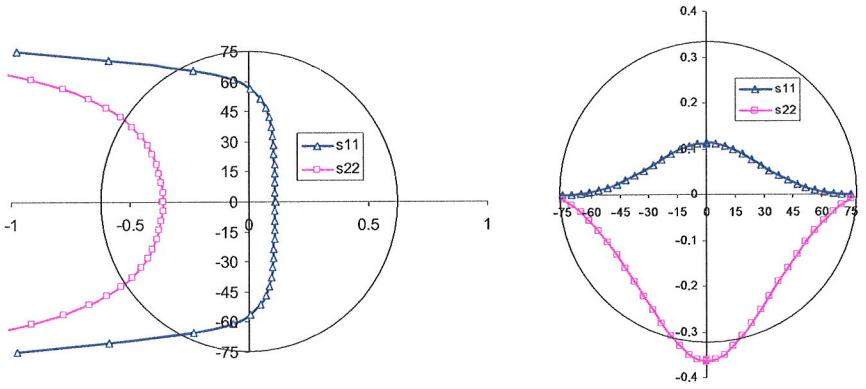

Figure 1. Elastic solution of stresses for IDT test

In order to study the viscoplastic material characteristics of asphalt mixture, a two-layer viscoplastic model was used to characterize the mixture behavior, serving as the basis for the numerical performance test. A macroscopic parametric study was conducted to obtain the sensitivity of each parameter to the deformation response of the sample. The sensitivity analysis will serve as a guide to calibrate the material model so that the simulation results can be matched with the actual test results. Finally, microscopic models for indirect tensile test and dynamic modulus test were built considering the viscous behavior of the asphalt binder or mastics and the phase configuration of the asphalt concrete mixture.

Asphalt concrete mixture shows temperature and time dependency under loading. Schapery (1984; 1990) introduced a model by replacing physical strains with pseudo strains so that a viscoelastic problem can be transformed into an elastic problem through the correspondence principle. Both monotonic loading and cyclic loading were investigated using this theory (Park et al. 1996; Zhang et al. 1997; Lee and Kim 1998a). Rate dependency of asphalt concrete makes is sensitive to loading and boundary histories. Integral description has to be used in material models that satisfy homogeneity and superposition principles. Furthermore, viscoplastic models were also introduced recently to describe the rate dependent plastic stress -

strain relationship. Collop et al. (2003) implemented an elasto-viscoplastic constitutive model with damage for asphalt. It was formulated based on the generalized Burger's model: an elastic element in series with a viscoelastic (Voigt) element (linear) and a viscoplastic element (nonlinear). A power law function was assumed for the viscoplastic strain rate-stress relationship. Damage was accounted for by introducing parameters that modify the viscosity. Tashman et al (2005b) developed a microstructure viscoplastic continuum model for asphalt concrete. The viscoplastic strain rate was defined using Perzyna (1966) flow rule and the linear Drucker-Prager yield function. The aggregate anisotropy was accounted for by introducing a microstructure tensor reflecting the orientation of non-spherical particles. Seibi et al (2001) used a Perzyna type viscoplastic constitutive model with isotropic hardening and Drucker-Prager yield criteria. Schwartz et al (2002) developed a model based on the extended viscoplastic Schapery continuum damage model. Time-temperature superposition was assumed to be valid in this model. It was concluded in their study that the assumption of time-temperature superposition is valid for both viscoelastic and viscoplastic strain responses.

Besides these models based on strain decomposition, Kichenin et al (1996) proposed a model with two-dissipative mechanisms, associating an elastic-viscous and an elastoplastic model in parallel. The model was used to simulate a cyclic pressure test on a pipe specimen. The model coefficients were calibrated with a single uniaxial test. This model can identify residual strain for relaxation simulation. The yield limit plays an important role for the description of the early stage deformation response to the loading. This stress overlay based model reflects the stress transfer between the two mechanisms and is suitable to describe materials consisting of multiple constituents. Based on the stresses obtained from this solution and the strains from the deformation measurement of the indirect tensile test (SHRP, 1993), the elastic modulus and Poisson's ratio can be derived. Zhang et al. (1997) extended the elastic solution to viscoelastic one and used the indirect tensile test to characterize viscoelastic material parameters. However, the viscoelastic solution still did not account for the plastic contribution on the total strain response and only used the instantaneous and the recoverable part of the test results. In this part, the whole response of the testing will be used to characterize the viscoplastic material properties. Numerical indirect tensile test and dynamic modulus test with the same boundary conditions as the real physical test are performed in this part to conduct parameter sensitivity analysis and viscoplastic characterization of the asphalt concrete mixture. After this macroscopic study, the microstructure of the asphalt concrete sample is introduced into the model to build realistic digital specimen and digital tests that enables the characterization of mixture properties as well as properties of individual material.

Also, a simulation model using asphalt mastic microstructure obtained from micro computed tomography (CT) scanning was built to capture the specific phase configuration. The combination of x-ray tomography imaging and finite element simulation provides an alternative for material characterization and a profound understanding of the behavior of composite materials (Wang et al. 2001; Zhang et al. 2005a,b; Zhang et al. 2006). In previous studies, methods were developed to link the material response to the sample microstructure, which was

characterized through x-ray tomography imaging. Programs were developed enabling the mapping of real microstructure into finite element simulation model. The back calculation based on the sensitivity analysis of material parameters were also carried out in a macroscopic statistic manner. The simulation successfully captured material performance qualitatively for different composite configurations, e.g., layered wood panels or asphalt mixtures, with different aggregate gradations or air voids volume fractions.

In order to further verify the algorithms and procedures with laboratory test, small asphalt concrete samples were prepared with different aggregate volume fractions in order to be X-ray scanned. The goal was to study the effect of aggregate volume fraction on the behavior of the sample and to further develop the concept and verify the algorithm and method. A material testing stage was used to conduct uniaxial compressive test on the mastic samples.

2. MACROSCOPIC STUDY

Finite Element Model

Indirect Tensile Test

Finite element geometry models were built to reflect the actual displacement and traction boundary of the specimen. Due to the symmetrical geometry of the whole specimen, only a quarter of the sample was modeled with proper boundary conditions (Figure 2). The location of the displacement measurement point was determined according to actual testing configurations for a sample of six inch diameter.

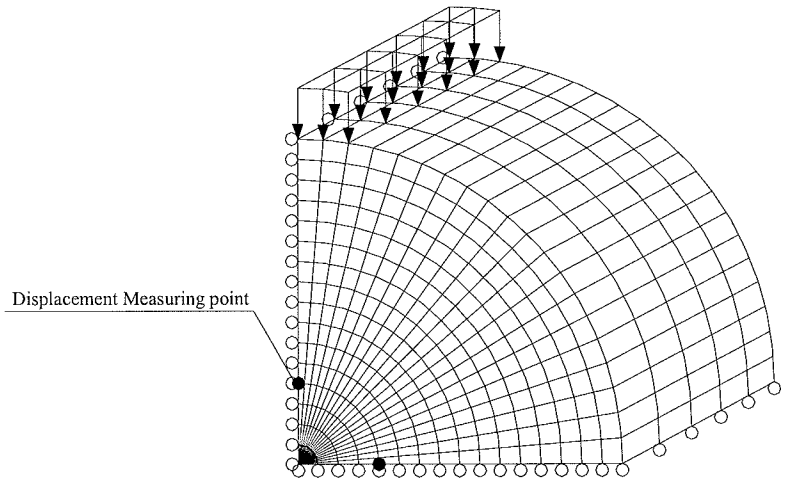

Figure 2. Geometry model of simulation IDT test

In the actual indirect tensile test, the boundary is applied by loading strips. Since the modeling of loading strips will involve contact problems, which is very time-consuming in the simulation, the

numerical model uses distributed traction force to represent the loading. At the symmetrical axis, a roller support boundary is applied to each node (Figure 2).
The loads are modeled as distributed boundary traction with repeated haversine pulse on a width of 3/8 inch for the entire thickness of the sample. The load amplitude and frequency were set to be the same magnitude and frequency as in the actual testing procedure (Figure 3).

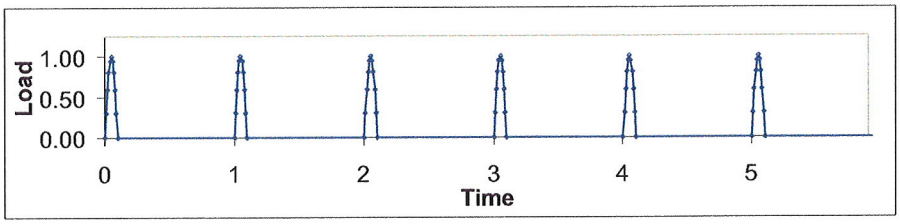

Figure 3. Indirect tensile test pulse loading

Dynamic Modulus Test

The simulation model of the dynamic modulus test is shown in Figure 4. Due to the axi-symmetric configuration of the macroscopic model, a four node bilinear axi-symmetric solid element with reduced integration and hourglass control was used. Similar to the indirect tensile test, the surface traction was used as loading instead of loading plate to avoid the involvement of contact problem.

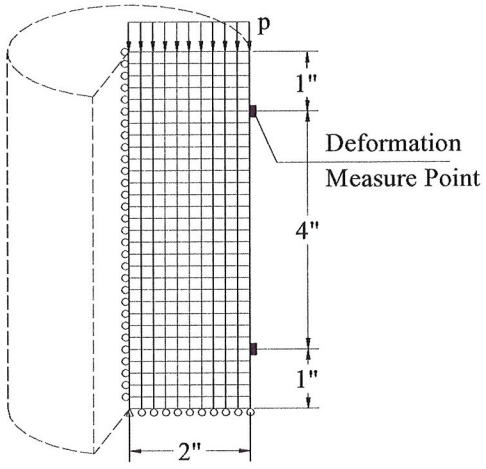

Figure 4. Finite element model for dynamic modulus test

The loads are modeled as distributed boundary traction with sinusoidal repetition (Figure 5) on the top edge of the sample.

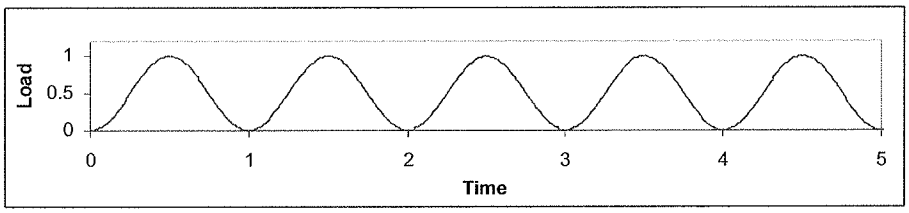

Figure 5. Dynamic modulus test sinusoidal loading

For both numerical tests, the cumulative deformation histories of the repeated loading simulation were recorded against loading time.

Material Model

The stress overlay based two layer viscoplastic model was used to describe the constitutive relationship of the asphalt concrete mixture in the macroscopic study and asphalt binder only in the microscopic study. The concept of this parallel network model is illustrated in Figure 6.

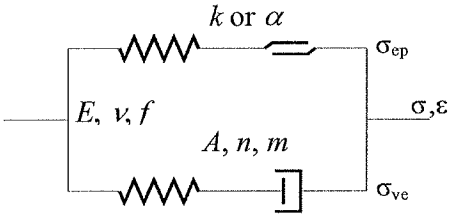

Figure 6. Two layer viscoplastic model

The total stress and strain in the networks can be expressed as equations (1)1).

$$\sigma = \sigma_{VE} + \sigma_{EP}$$
$$\varepsilon = \varepsilon_{EP} = \varepsilon_{VE} \quad (1)$$

where subscript $_{VE}$ represents the viscoelastic network and $_{EP}$ represents the elastoplastic network, f is the stiffness ratio of the viscoelastic network and is expressed as equation (2) (2).

$$f = \frac{K_{VE}}{K_{EP} + K_{VE}} \quad (2)$$

where K is the instantaneous modulus. The von Mises type plasticity was used in the elastoplastic component. The flow rule is expressed in equations (3).

$$\dot{\varepsilon}'_{ij} = \frac{1}{2\mu} S_{ij} + \frac{1-2\nu}{E} \sigma_{ij} \delta_{ij}$$

$$\dot{\varepsilon}''_{ij} = \dot{\bar{\varepsilon}}^{pl} \cdot \frac{3}{2} \frac{S_{ij}}{q} \tag{3}$$

$$q = \sqrt{\frac{3}{2} S_{ij} S_{ij}}$$

The strain hardening type creep law was used. It is expressed as equations (4) (ABAQUS, 1995).

$$\dot{\varepsilon}''_{ij} = \dot{\bar{\varepsilon}}^{cr} \cdot \frac{3}{2} \frac{S_{ij}}{q}$$

$$\dot{\bar{\varepsilon}}^{cr} = \left(A q^{n} \left[(m+1) \bar{\varepsilon}^{cr} \right]^{m} \right)^{\frac{1}{m+1}} \tag{4}$$

$$q = \sqrt{\frac{3}{2} S_{ij} S_{ij}}$$

where $\dot{\bar{\varepsilon}}^{cr}$ is the uniaxial equivalent creep strain rate, ε^{cr} is the uniaxial equivalent creep strain, S_{ij} is the deviatoric stress tensor, q is the uniaxial equivalent deviatoric stress, and A, n, m are material constants.

There are seven parameters need to be calibrated. They are: elastic modulus E, Poisson's ratio ν, modulus ratio f, viscous parameters A, m, n, and the initial yield stress σ_{yp}.

Numerical Experiment

The simulation was conducted on the Supercomputer at the High Performance Computing facility at Virginia Tech. The Inferno2 computing system uses parallel computing technology that provides high speed as well as large disk space and memory. Simulations of the indirect tensile test were conducted using the model in ABAQUS with the repeated half sine pulse loading and cumulative deformation was obtained for each time increment. This historic deformation pattern is used together with the experimental counterpart to carry out parameter calibration.

The stress distributions along diameters are plotted in Figure 7. They are almost the same for the elastic solution and the viscoplastic simulation. However, the total displacement is apparently different. Figure 8 shows the vertical displacement recorded along the vertical diameters for the elastic solution and the viscoplastic simulation. The total displacement response of the sample is used to calculate the material parameters for the elastic, viscous and plastic components.

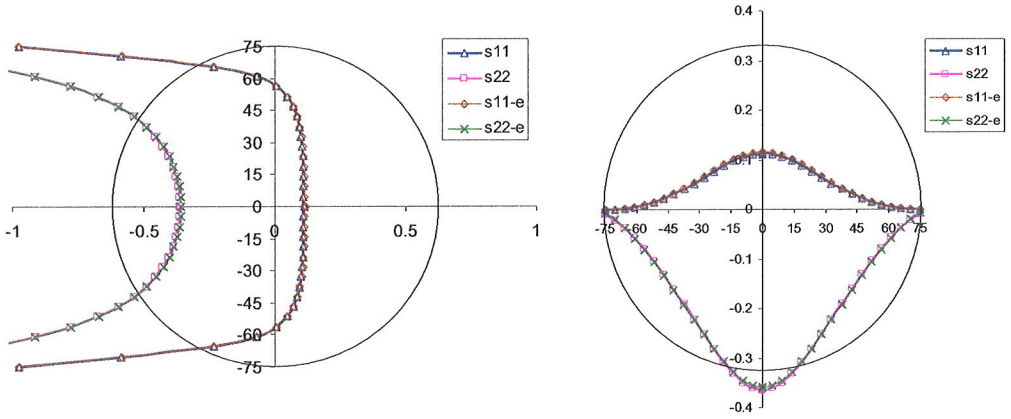

Figure 7. Stress distributions for elastic and viscoplastic solutions

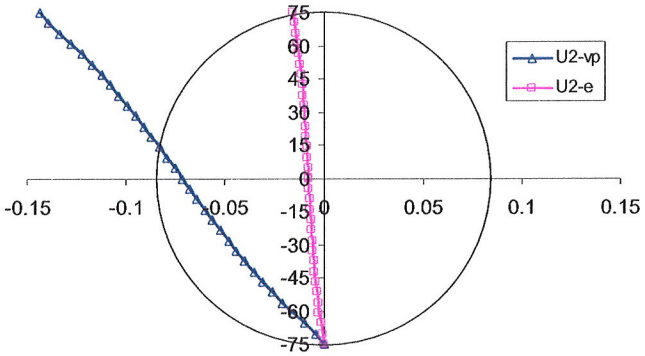

Figure 8. Displacement for elastic and viscoplastic solutions

Physical Experiment

Some results of indirect tensile tests and dynamic modulus tests conducted at Virginia Tech Transportation Institute were used in this study for comparison with the simulation results. In the indirect tensile test, a controlled stress was applied and deformations along both the vertical diameter and the horizontal diameter were measured and recorded as historical outputs. These deformations were measured at the center sections of both diameters with the sector length of 0.25D (D is the diameter of the sample). The setup of the test is illustrated in Figure 9. However, the test only recorded final part of the cumulative data, which made it difficult to use to characterize the model parameters. Due to this reason, the results of dynamic modulus test were used instead. The test setup for the dynamic modulus test is also illustrated in Figure 9. Measurement points are located four inches apart along the sample and three sets of them are

mounted on each sample. Test results at 5°C and 40°C were used to back calculate material parameters for three dimensional (3D) stress conditions.

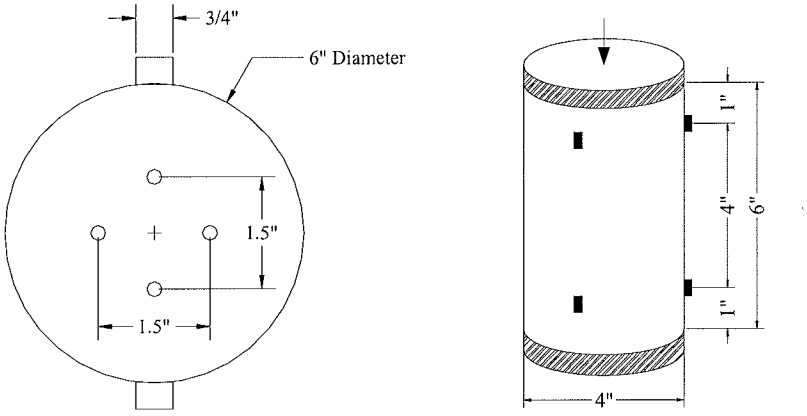

Figure 9. Specimen loading for indirect tensile test (left) and dynamic modulus test (right)

Parameter Back Calculation

The parameters of the material model were obtained by back calculation using the simulation results and the testing data. The concept is to obtain a set of parameters that render closest deformation profile to the testing results. In this study, the objective function is taken as equation (5).

$$\sum_{i=1}^{N}(\delta_i^m - \delta_i^p)^2 \qquad (5)$$

where N is the number of time points for the deformation history, δ_i^m, δ_i^p are measured and predicted final deflection values respectively. The instantaneous response was used to estimate the elastic modulus and the stiffness ratio between the two mechanisms.

Sensitivity Analysis

A sensitivity analysis for each independent material parameter was conducted before the optimization. The sensitivity is an input of the estimation process. Three steps were taken in the calibration procedure. In the first step, an initial simulation profile was obtained with a set of parameters that are typical values for asphalt concrete mixtures. In the second step, sensitivity analysis of each parameter was conducted to find the effect of each parameter to the simulation results. The third step included a series of simulations carried out to obtain the set of parameters leading to the minimization of the objective function.

There were seven parameters in the two layer viscoplastic model used in this study. However, in order to simplify the procedure, some of the parameters that have less sensitivity were fixed at typical values. Poisson's ratio was taken as 0.3 for both networks and linear

hardening was assumed for the elastoplastic network, reducing the number of parameters to six.

The elastic modulus and the stiffness ratio of the viscous part can be obtained from the instantaneous response of the deformation profile. They not only affect the instantaneous part of the response, but also the permanent deformation and should be adjusted with the long term response profile. Other parameters mainly affect the plastic part of the response. The effect of each parameter on the final deformation is plotted in Figure 10 and the percentage change of the deformation caused by 10% change of each individual parameter is listed in Table 1. Among them, the parameter A, m and σ_{yp} have major effects on the permanent deformation profile. A sensitivity study was also performed in the macroscopic simulation.

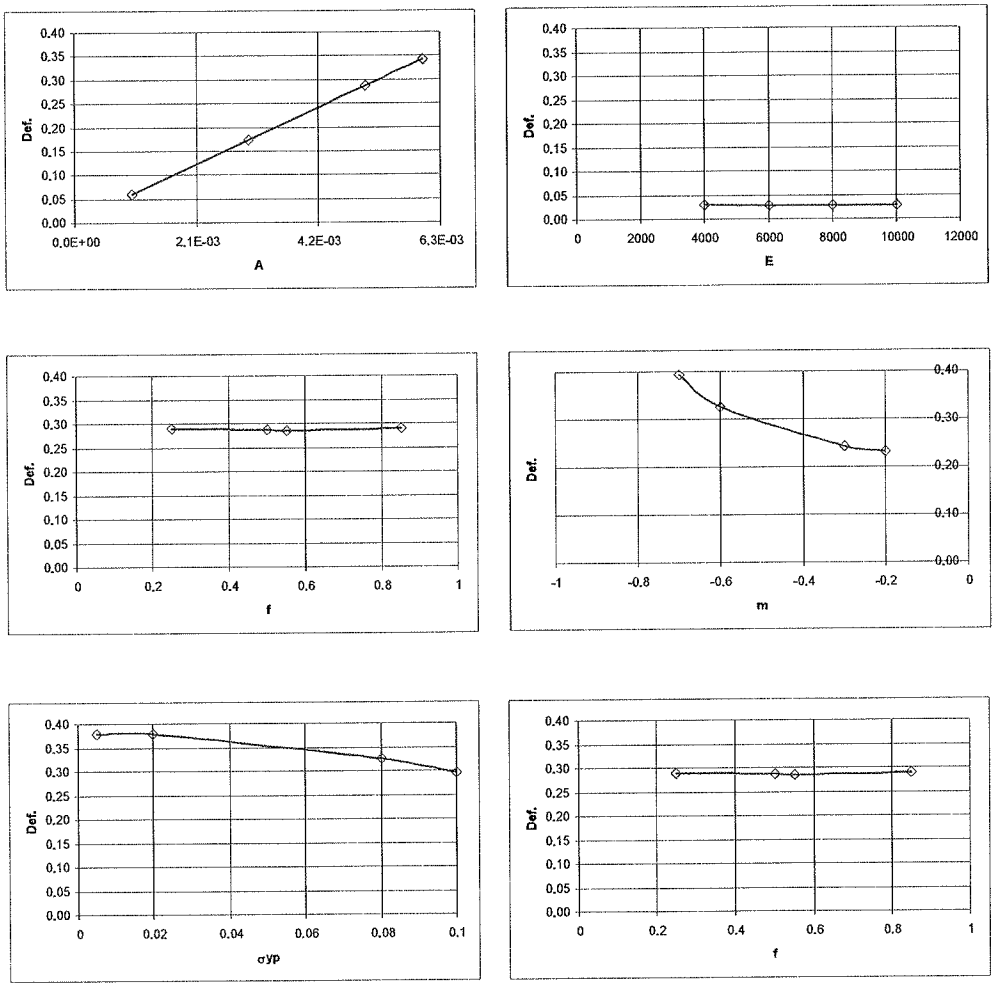

Figure 10. Parameter sensitivity to deformation profile

Results from the sensitivity evaluation of each parameter are presented in Figure 11 and Figure 12. Based on the macroscopic simulation results and the testing data, the parameters in the material model were obtained following the optimization procedure above using the sensitivity analysis results as a guide.

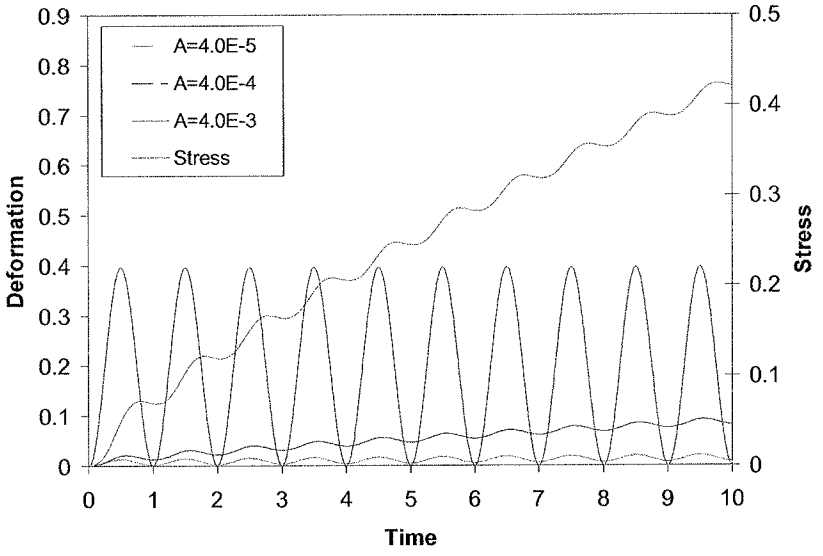

Figure 11. Effect of parameter A on the displacement profile of numerical dynamic modulus test

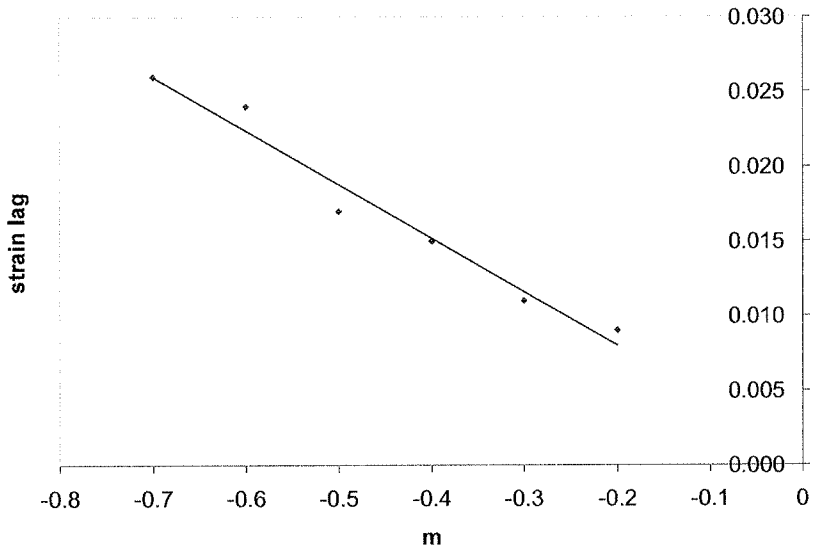

Figure 12. Effect of parameter m on the phase angle for numerical dynamic modulus test

Table 1. Percentage change of deformation caused by 10% change of parameters

	Initial Parameter	Average Percentage Change from 10%
E	6000	1.06%
ν	0.35	
σ_{yp}	0.08	0.04%
A	0.005	9.76%
f	0.55	0.28%
m	-0.2	3.41%
n	0.6	3.60%

The simulated deformation profile and the actual testing records are plotted against time, as shown in Figure 13 and 14, based on the optimized material parameters from Table 2. From both deformation profiles, the dynamic modulus and the phase angle for each testing frequency can be obtained. The testing results were normalized for the sole purpose to calculate the dynamic modulus and phase angle instead of recording of the entire deformation profiles along with the loading history. The testing temperatures were 5°C and 40°C, respectively. Figure 15 and 16 show the effects of stiffness ratio parameter *f*, on the lag of strain response and the magnitude of the response, respectively.

Table 2. Optimized material parameters used for simulation

Parameters		5°C	40°C
E	(N/mm^2)	30,000	4,100
ν		0.3	0.35
σ_y	(N/mm^2)	0.08	0.08
σ_u	(N/mm^2)	0.8	0.8
ε_u		0.6	0.6
A		1.0E-06	4.0E-05
n		0.8	0.8
m		-0.2	-0.2
f		0.85	0.85

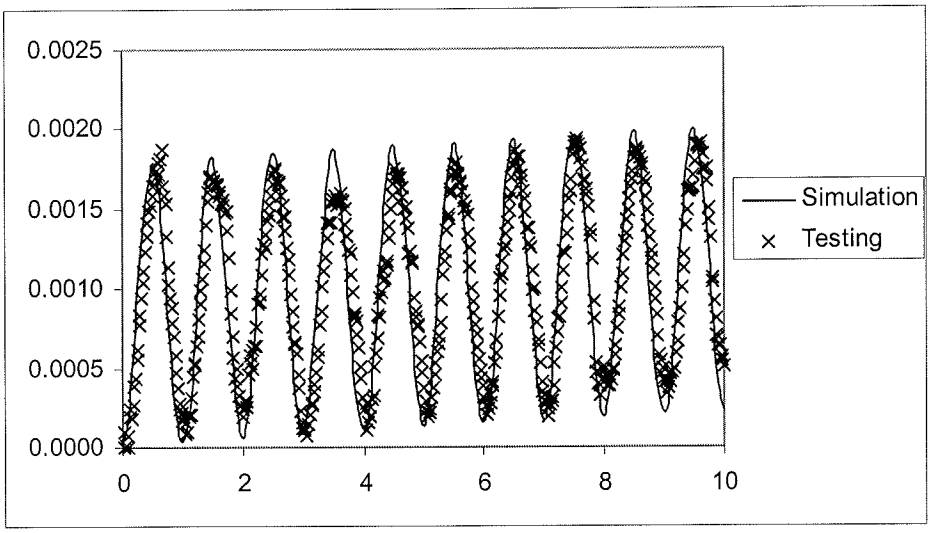

Figure 13. Simulation and experimental result at 5°C for macroscopic dynamic modulus testing, an actual test with 1Hz frequency was used

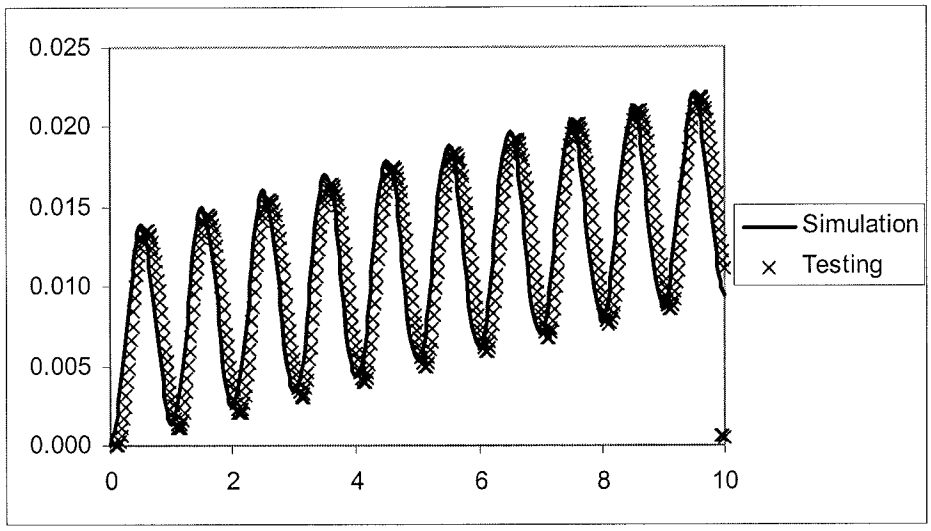

Figure 14. Simulation and experimental result at 40°C for macroscopic dynamic modulus testing, an actual test with 1Hz frequency was used.

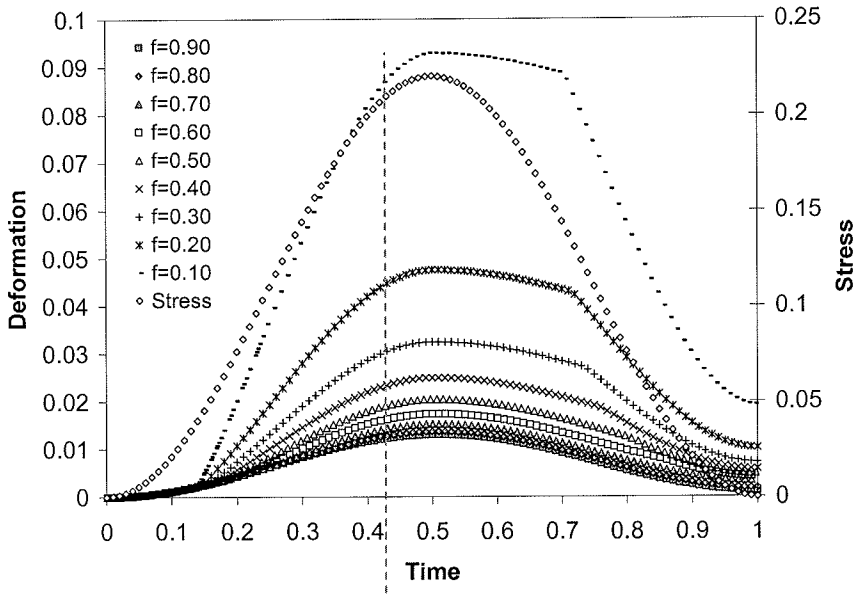

Figure 15. Deformation variation for parameter f ($0 < f < 1.0$), the plot shows the effect of the parameter f on the phase angle

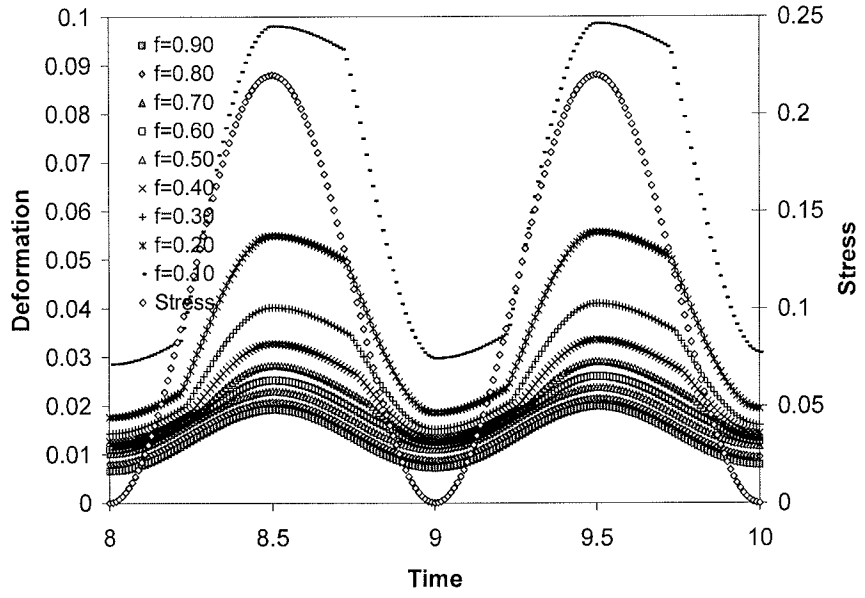

Figure 16. Steady state deformation variation for parameter f ($0 < f < 1.0$), plot shows the effect of parameter f on the dynamic modulus

3. MICROSCOPIC STUDY

Three dimensional microscopic models were built for the indirect tensile test and dynamic modulus test considering phase variation of different mixtures to achieve the final stage of development, the digital specimen and the digital test functionality. The microstructural information is from the x-ray scanning of the actual sample. Linear elastic material model was used for aggregates, while the two layer viscoplastic material model was used for asphalt binder. The voids are removed before the application of the repeated loading. The loading is applied through the form of boundary traction. The displacement of the loading point is monitored and the displacement history is recorded along with the loading history. Due to computing time and the limitation of the computer memory and disk space, especially for repeated loading simulation, all the images with original 512×512 resolution were re-digitalized before the building of the finite element model. This was done by maintaining the volume fractions of both the voids and aggregates during the conversion. A FORTRAN program was developed to carry out the conversion of the microstructure and the generation of the finite element model (see Figure 17).

In order to validate these concepts, mixtures from the WesTrack project were numerically tested with the procedure developed above. Three mixtures were subjected to the same loading pattern and magnitude so that we could obtain comparable deformation responses for different mixtures. The results plotted in Figure 18 indicate different strain responses for different mixtures with the same material properties for each component. The graph shows the deformation history of the three mixes mentioned before. The fine-plus mix, as expected, demonstrated larger deformation than the fine mix. However, the coarse mix experienced less deformation than the fine plus mixture. This may be due to the selection of material parameters and the interpretation of the phases from scanning images based on volume fractions. The loss of accuracy when converting images from high resolution to low resolution was minimized by keeping consistent phase fractions. Meanwhile, three levels of re-digitalization are conducted and numerically tested with the same material model and same set of material parameters. The simulation of five loading cycles with the same sample size and loading pattern were obtained (Figure 19). The parameters were calibrated using the back-calculation method which was conducted later following the same approach as in the macroscopic study illustrated previously. As for the time history, the difference in the deformation for these three mixes increased with the increase of the loading cycles. This shows the importance of the sample microstructure when dealing with large number of cycles of repeated loading which is the real situation of asphalt pavement.

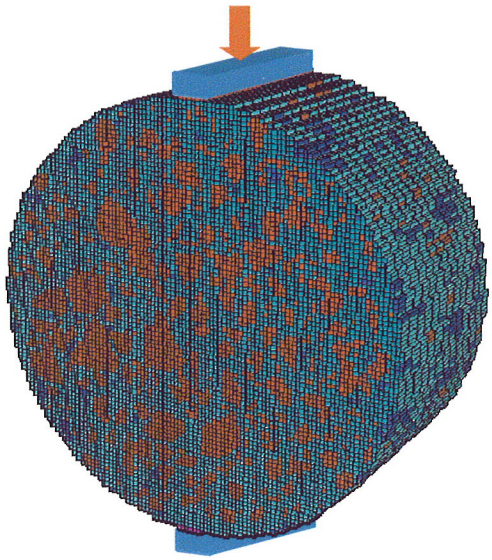

Figure 17. Microscopic finite element model for the indirect tensile test

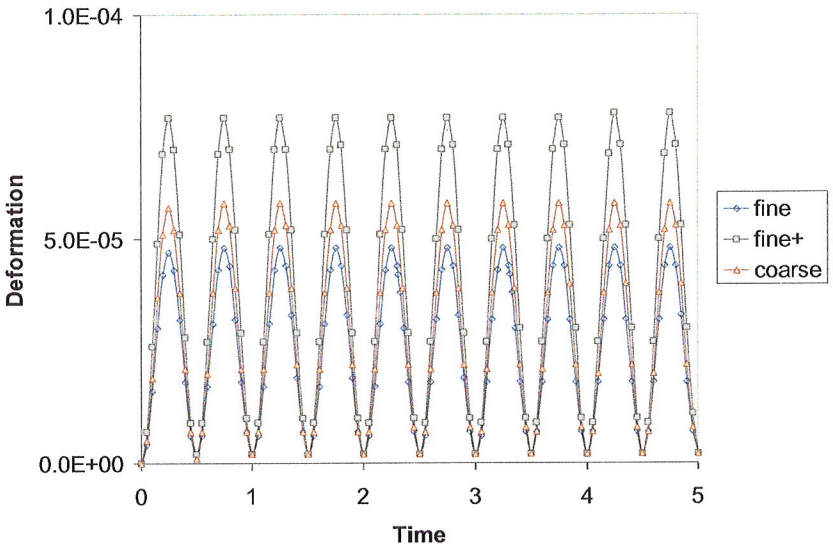

Figure 18. Microscopic numerical testing of samples from WesTrack mixtures

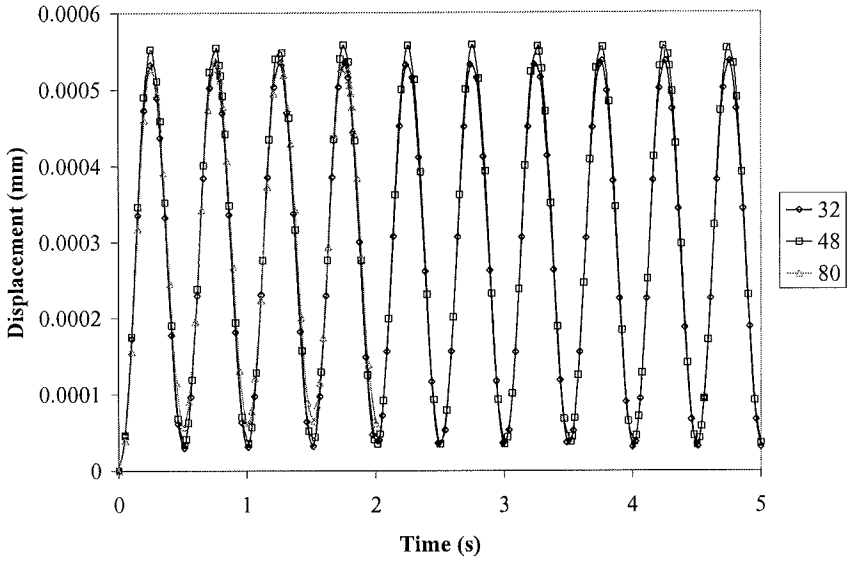

Figure 19. Displacement profile for mesh size 5mm, 3mm, and 2mm

The dynamic modulus test of the same sample can be achieved by changing the loading boundary and direction. A uniaxial load is applied along the main axis of the sample instead of its diametrical axis. The systematic study on dynamic modulus test is currently being carried out with the image re-digitalization and mesh refinement methods.

Asphalt Samples Scanning and Test Simulation

Eight test samples were prepared in total. Two were pure asphalt binder and six were mastics containing fine aggregates with the following volume fractions: 5%, 25%, and 50%. All samples were cylindrical with 6mm in diameter and 9mm in height. They were poured in an aluminum mould specially designed for small asphalt and mastic samples. The actual aggregate volume fractions may have be different from the above values due to the presence of air voids, as they are difficult to control for this kind of small samples. The actual volume fractions and air voids were quantified through 3-D image analysis of the reconstructed sample. Aggregates passing the No.16 sieve and retained on the No.30 sieve (i.e., 0.6 ~ 1.18mm) were used for all samples. Table 1 shows the aggregate-asphalt ratio for different aggregate contents.

Table 3. Aggregates to binder weight ratio for different volume fractions

Aggregate fraction (%)	100	50	25	5
Weight ratio	n/a	2.65:1	1:1.15	1:7.5

The volume fractions of aggregates and air voids of the samples are listed in Table 4. These values are used to generate the finite element models.

Table 4. Volume fraction (%) of aggregates and air voids

Sample ID		2a	2b	3a	3b	4a	4b
Volume fraction	Aggregates	5.87	4.04	22.42	23.49	50.52	49.91
	Voids	3.48	1.18	1.77	2.46	12.97	11.26

For these small samples, the air void fractions are closely related to the aggregate contents. If more samples were to be made, an accurate relationship between the volume fractions of these two phases could be developed. This implies that the air void contents can be predicted from the aggregate contents based on a statistical analysis of the results from the 3-D image analysis. However, other factors, such as the shape and gradation of the aggregate may affect the volume fraction relationship.

X-ray Scanning

Skyscan1174 microtomographic system and materials testing stage MTS-50N were used in this study to obtain the microstructure imaging of the samples and to conduct uniaxial compressive test. They are pictured in Figure 20. The scanner x-ray source is 20-50 kV with a maximum power of 40 W and a spatial resolution of 6 to 30 μm. The material testing stage can perform compression, tension and torsion test. All samples were scanned before testing them in compression at 512 x 512 resolution. Volumetric reconstruction of the scanned samples was performed to create their three-dimensional models. The models were further analyzed to determine the volume fractions for aggregates, binder and air voids. Subsequently, data from the 3-D analysis were used to obtain threshold values necessary for generation of the finite element models.

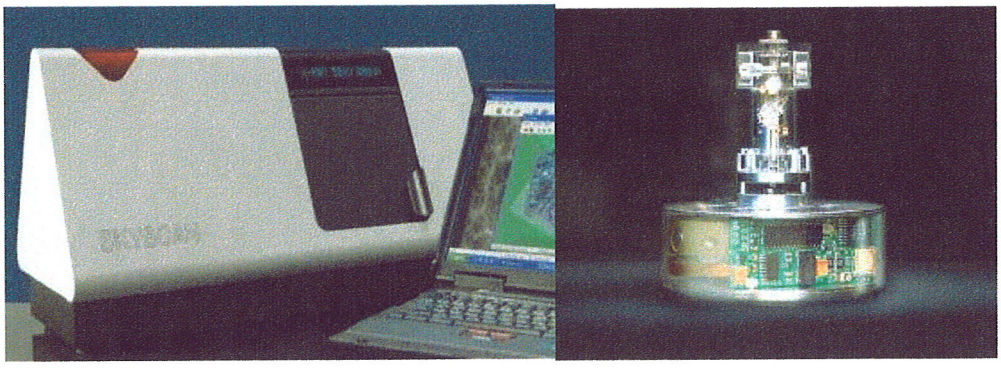

(a) (b)

Figure 20. X-ray scanner (a) and material testing stage (b)

Images of scanned mastic samples (inside the testing stage) as well as reconstructed cross-section are showed in Figure 21. The height of the sample can be measured on the screen (vertical red line) using software features. In the reconstructed slice the white spots represent the aggregates.

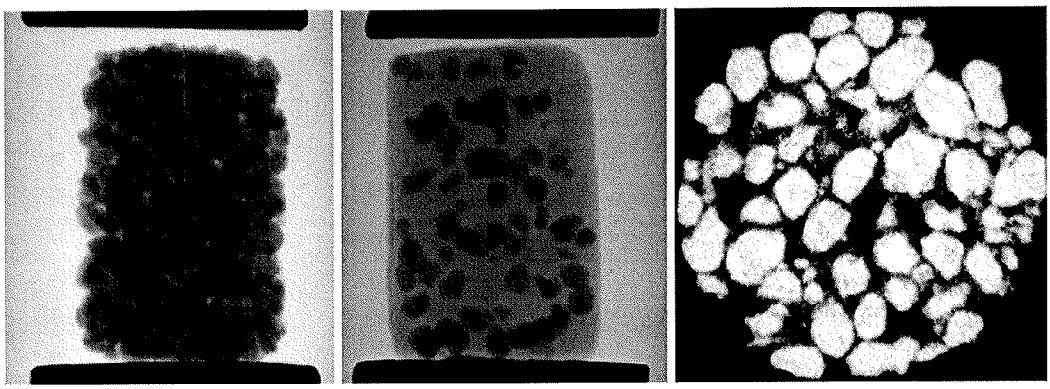

Figure 21. Samples with different aggregate volume fraction during scanning (left) ~50% aggregates, (center) ~5% aggregates and (right) reconstructed section image

Reconstructed cross-sectional images were read with programs developed in Interactive Data Language (IDL) and transferred into a data file read by a FORTRAN program to generate an input for the finite element model. In this study, adaptive meshes were used for asphalt binder to account for large distortions that may occur within thin asphalt layers between two aggregates.

Uniaxial Compression Test

The MTS-50N testing stage (Figure 20b) is displacement controlled and applies symmetrical loading from above and below the sample in uniaxial compression. Prior to each test, the stage had to be calibrated according to the manufacturer requirements. They included a speed of 16 μm/s and a load force of 0.22N. Testing was manually stopped when the applied force reached 22.6N because of simulation reasons. All samples were tested at room temperature and their lengths (heights) were measured on screen before testing. The total displacement recorded varied from 1mm to 3mm. However, due to severe deformation of the mastic sample during testing, which increased the sectional area, only the beginning part of the test results curve was used for finite element simulation and back calculation of material parameters.

Based on the force-displacement dependency from the testing of the pure binder sample, shown in Figure 22 (left), a stress-strain relationship was developed, from which elastic modulus, yield stress, and strain hardening were estimated. These properties were then used as initial parameters in the back calculation. After adding aggregates into the asphalt binder, the behavior of the composite material is significantly different from that of pure binder, especially for samples with higher aggregate volume fraction. However, samples with 5% aggregate volume

fraction only have slight difference with pure binder samples in terms of force-displacement response.

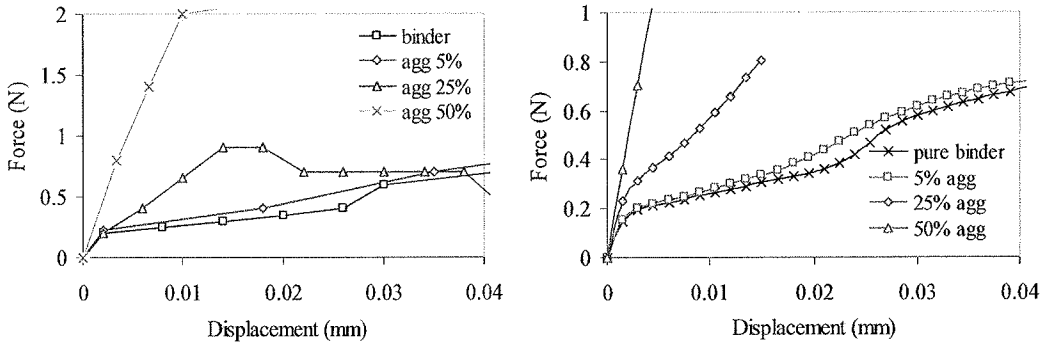

Figure 22. Force-displacement curves from actual tests (left) and test simulations (right)

Uniaxial Compression Test Simulation

The simulation of the dynamic modulus test was conducted as a small scale uniaxial compression test. The two-layer viscoplastic material model was used for asphalt binder and an elastic model was used for aggregates. Loading plates were modeled as rigid surfaces. The movement of the top and bottom rigid surfaces was set at 16μm/s, same speed as that in the physical test. Parameters in the material model were back calculated based on the parameter sensitivity study and they were calibrated from one set of samples. Then, the same set of material parameters was used in the simulation of other sets of samples with different aggregate volume fractions.

Three-dimensional models created from reconstructed samples representing different aggregate volume fractions are shown in
Figure 23. In this representation, the voids and binder were set to be partially transparent. Similarly, individual phases can be visualized separately. This is particularly useful in the study of void structure or connectivity.

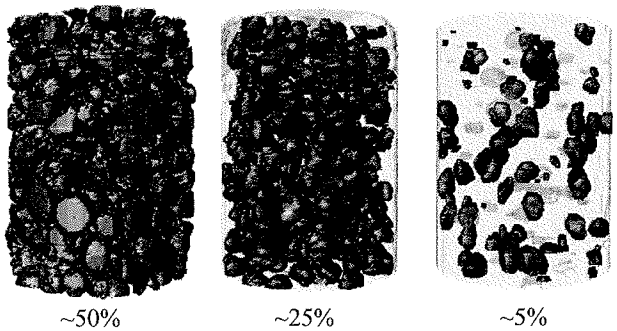

Figure 23. 3-D models of asphalt samples with different aggregate volume fractions: 50%, 25%, and 5%

The simulation of the uniaxial compression test was conducted at Virginia Tech's high performance computing facility which utilizes parallel computing and provides memory and disk space for large applications. The finite element model has approximately 30,000 elements with a mesh size small enough to capture the aggregates and voids and to reflect their effects on the deformation response. The simulative finite element models revealing the asphalt sample microstructures are shown in Figure 24.

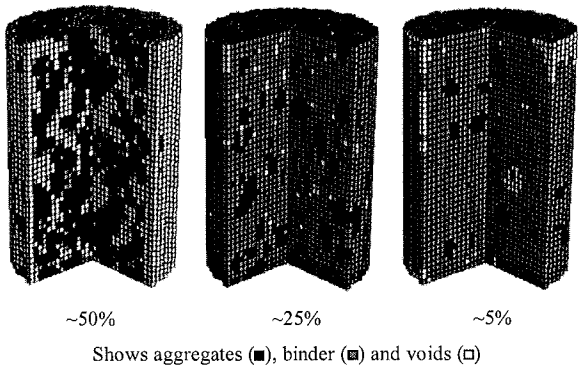

Figure 24. Finite element models of asphalt samples (one quarter of the digital sample was removed to show the internal microstructure)

Finite element models simulating the uniaxial compression test are pictured in Figure 25. They include the deformable sample part and both rigid loading surfaces. When comparing the aggregate configurations before and after loading from the outline plot it can be observed that some areas with much larger deformations are associated with aggregate rotation (after loading). They are usually in the vicinity of places with high concentration of voids.

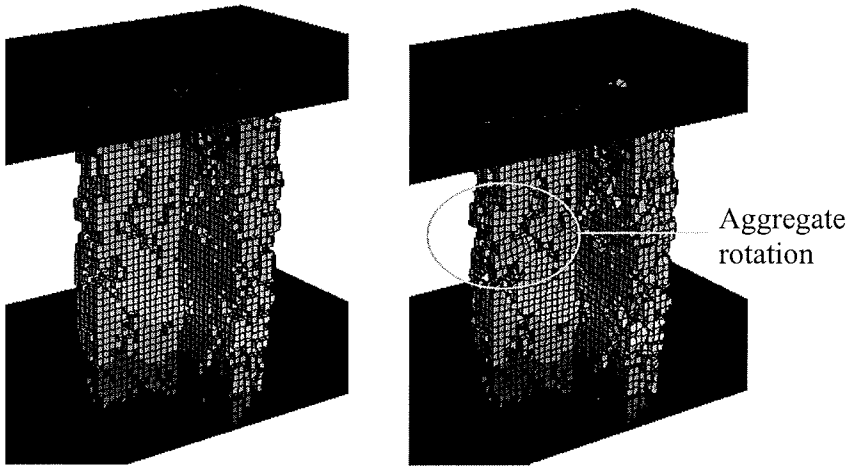

Figure 25. Finite element simulation models of the uniaxial compressive test of asphalt samples: before loading (left) and after loading (right)

From the stress-strain dependency established during testing of the pure binder sample, initial material parameters for the finite element simulation were obtained. These parameters were further optimized by minimizing the objective function within the ABAQUS environment. Material parameters obtained through back calculation are listed in Table 5. They were used in all the simulations of the mastic samples. Parameters for the elastic model used for aggregates were obtained by adjusting the parameters of elastic model for the mastic sample having 5% aggregate volume fraction. The back calculated aggregate parameters are also listed in Table 5. However, the viscoplastic material (asphalt binder and mastics) parameters remained unchanged during the optimization of the elastic part. This makes the model calibration relatively easier. The force-displacement simulation curves in Figure 22 (right) were generated using these parameters. All the back calculated parameters listed in Table 5 were used in the remaining simulations, i.e., for samples with aggregate volume fraction of 25% and 50%.

Figure 26, showing the simulation results versus testing results, indicates the validity of the developed evaluation method. It can be seen that the simulation results are in agreement with the test results, especially for samples with lower aggregate content. Thus, the material parameters obtained from pure binder test sample and mastic with 5% aggregate are able to be used in simulating testing of samples with different aggregate contents but same material properties. This means that material parameters obtained from individual material tests could be used in simulating tests of composite materials incorporating their actual microstructure. In this case, the real microstructural configuration is very important in the simulative tests of composite materials besides the properties of the individual components. In both, the physical and simulative tests, the stiffness of asphalt binder is fairly small compared to samples with aggregates. This is due to the lack of aggregates' interlock action that is partially enhanced by the asphalt binder. The stiffness of each sample was calculated at a displacement of 0.01mm for both physical and simulative test results.

Table 5. Material parameters from back calculation

Parameters			Back calculated values
Asphalt binder	E	(N/mm^2)	31.83
	ν		0.45
	σ_y	(N/mm^2)	0.0070736
	σ_u	(N/mm^2)	0.028294
	ε_u		0.004
	A		1.0E-6
	n		0.8
	m		-0.18
	f		0.85
Aggregates	E	(N/mm^2)	210
	ν		0.167

The dependency between stiffness and aggregate volume fraction, shown in Figure 27, indicates a possible correlation of stiffness with aggregate content. It also indicates an increased rate of stiffness with the increase of aggregate volume fraction.

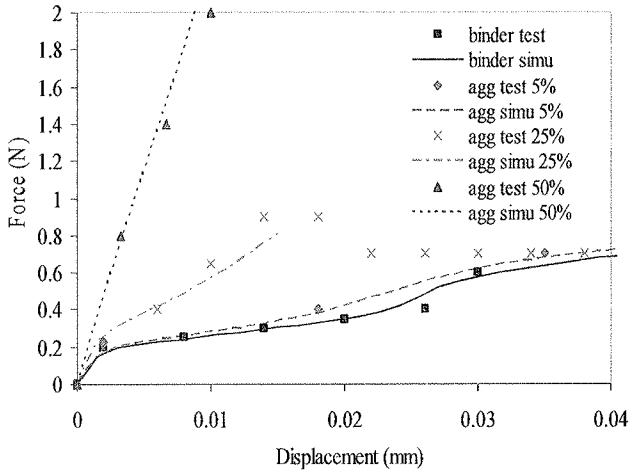

Figure 26. Simulation results with calibrated material parameters versus testing results

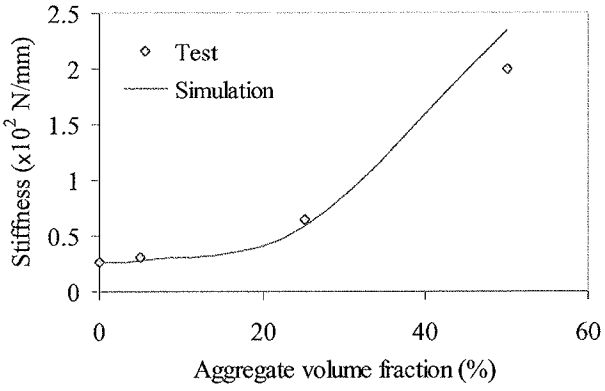

Figure 27. Stiffness vs. aggregate volume fraction for asphalt samples at 0.01mm deformation

4. CONCLUSIONS

Based on the laboratory testing, analysis of test data, and finite element simulation, the following conclusions can be drawn.

• The digital specimen and digital test techniques have been proved to be a valid technology for the characterization of asphalt concrete. Even using simple material models (for example, elasticity), the incorporation of the microstructure of materials have added another dimension in assessing or differentiating asphalt mixes.

• Compared with the experimental results, the rate dependent material model for asphalt binder renders qualitatively realistic simulation of the responses of asphalt mixtures.

• The model mesh size affects the simulation results in terms of elastic stiffness of the deformation response. Coarse meshes will generally lead to a stiff deformation response. However, due to the effects of the microstructure of the sample, softening may be observed with the configuration of the voids and aggregates.

• Material parameter estimation can be acquired from parameter back calculation based on the simulation results, testing data and sensitivity analysis. Based on this estimation, the viscoplastic model for asphalt binder can be further refined/ simplified.

• The viscoplastic model should include a damage parameter to characterize the softening part after the peak strength.

• On the overall, the digital specimen and digital test technique is promising and should be further refined and implemented. Two limitations (image processing to convert gray images into binary images, and computational efficiency) should be removed before full implementation can be achieved.

5. RECOMMENDATIONS AND FUTURE WORK

• Currently, the digital test is run on a commercial FEM platform ABAQUS, which is very powerful but requires licensing fee and significant training of users. The programs to perform image processing and digital specimen constructing are built on other platforms. There is a need to combine these two into one platform with simple 'clicking button' options so that it is easy to use and the training can be minimized.

• Currently, binary images are used to build the digital specimens. While resolutions in representing the microstructure of the material are higher, the computational efficiency has decreased. Pre-processing of the gray images and homogenization of the material properties may enhance the computational efficiency.

• Develop a Type II proposal for the IDEA program to obtain additional fund to achieve the objectives of the above two recommendations.

• Work tightly with the Turner-Fairbank research center to implement the Type II development.

• After initial implementation at Turner-Fairbank, efforts should be made towards developing a pooled fund study to widely implement the technology.

While a Type II proposal was submitted to the IDEA program in September 2008 and the decision is pending, the research team has been using its own resources to develop a combined platform independent of commercial programs. Figure 28 illustrates some of the functions.

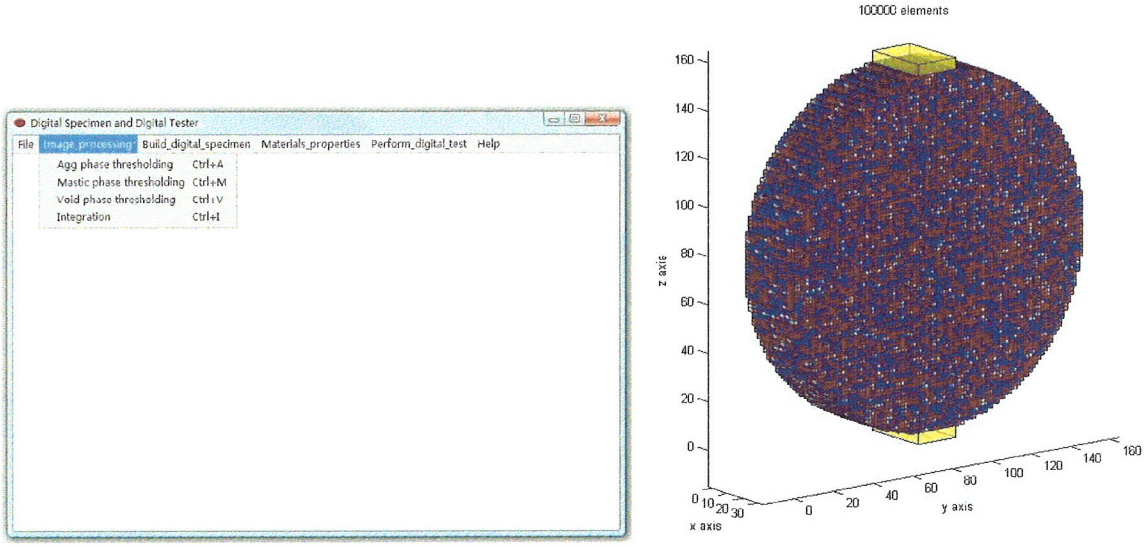

Figure 28 The Combined Digital Specimen and Digital Tester Program

REFERENCES

ABAQUS (1995). "User's Manual." Hibbitt, Karlsson & Sorensen, Inc., Pawtucket, R.I.

Collop, A. C., Scarpas, A. T., Kasbergen, C. and Bondt, A. d. (2003). "Development and Finite Element Implementation of a Stress Dependent Elasto-visco-plastic Constitutive Model with Damage for Asphalt." TRB 2003 Annual Meeting CD-ROM.

Hondros, G. (1959). "Evaluation of Poisson's Ratio and the Modulus of Materials of a Low Tensile Resistance by the Brazilian (Indirect Tensile) Test with Particular Reference to Concrete." Australia Journal of Applied Science **10**(3), p. 243-268.

Kichenin, J., Van, K. D., and Boytard, K. (1996). "Finite-element Simulation of a New Two-Dissipative Mechanisms Model for Bulk Medium-density Polyethylene." Journal of Materials Science **31**(6), p. 1653-1661.

Lee, H. J. and Kim, Y. R. (1998). "Viscoelastic Constitutive Model for Asphalt Concrete under Cyclic Loading." ASCE Journal of Engineering Mechanics **124**(1), p. 32-40.

Park, S. W., Kim, Y. R. and Schapery, R. A. (1996). "A Viscoelastic Continuum Damage Model and Its Application to Uniaxial Behavior of Asphalt Concrete." Mechanics of Materials **24**(4), p. 241-257.

Perzyna, P. (1966). "Fundamental Problems in Viscoplasticity." Advances in Applied Mechanics **9**, p. 244-368.

Schapery, R. A. (1984). "Correspondence Principles and a Generalized J-integral for Large Deformation and Fracture Analysis of Viscoelastic Media." Intl. Journal of Fracture **25**(3), p. 195-223.

Schapery, R. A. (1990). "A Theory of Mechanical Behavior of Elastic Media with Growing Damage and Other Changes in Structure." J. Mech. Phys. Solids **38**, p. 215-253.

Schwartz, C. W., Gibson, N. H., Schapery, R. A. and Witczak, M. W. (2002). "Viscoplasticity Modeling of Asphalt Concrete Behavior." ASCE Geotech. Special Publ., **123**, p. 144-159.

Seibi, A. C., Sharma, M. G., Ali, G. A. and Kenis, W. J. (2001). "Constitutive Relations for Asphalt Concrete Under High Rates of Loading." Transp. Res. Rec. **1767**, p. 111-119.

SHRP (1993). "Resilient Modulus for Asphalt Concrete." SHRP Test Designation: AC07, Protocol: P07.

SKYSCAN 1174 (2006). SkyScan 1174 Brochure, SkyScan Microtomography Manual.

Tashman, L., Masad, E., Zbib, H., Little, D. and Kaloush, K. (2005). "Microstructural Viscoplastic Continuum Model for Permanent Deformation in Asphalt Pavements." Journal of Engineering Mechanics **131**(1), p. 48-57.

Wang, L. B., J. D., Frost, and N. Shashidhar (2001). "Microstructure Study of Westrack Mixes from X-ray Tomography Images." TRR **1767**: 85-94.

Zhang, B., L. Wang, and M. Tumay (2006). "An Evaluation of the Stress Non-Uniformity Due to the Heterogeneity of AC in the Indirect Tensile Test." ASCE Geotechnical Special Publication, No. 146, p. 29-43.

Zhang, B., Q. Wu, L. Wang, and G. Han (2005a). "Characterization of Internal Void Structure of Strand-based Wood Composites using X-ray Tomography and Digital Tools." Proceedings of McMat2005: 2005 Joint ASME/ASCE/SES Conference on Mechanics and Materials, June 1-3, 2005, Baton Rouge, Louisiana, USA.

Zhang, B., Q. Wu, L. Wang, and G. Han (2005b). "The Influence of in-plane Density Variation on Engineering Properties of Oriented Strandboard: A Finite Element Simulation." Proceedings of McMat2005: 2005 Joint ASME/ASCE/SES Conference on Mechanics and Materials, June 1-3, 2005, Baton Rouge, Louisiana, USA.

Zhang, W., Drescher, A., and Newcomb, D. E. (1997). "Viscoelastic Analysis of Diametral Compression of Asphalt Concrete." ASCE Journal of Engineering Mechanics **123**(6): 596-603.